SOLUTION MINING RESEARCH INSTITUTE
105 Apple Valley Circle
Clarks Summit, PA 18411, USA

Telephone: +1 570-585-8092
Fax: +1 570-585-8091
www.solutionmining.org ◆ smri@solutionmining.org

Technical Conference Paper

Effect of natural convection on blanket dissolution rate in a salt cavern

Mehdi Karimi-Jafari, Ecole Polytechnique, Palaiseau, France
Pierre Bérest, Ecole Polytechnique, Palaiseau, France
Benoit Brouard, Brouard Consulting, Paris, France

Fall 2007 Conference
7-10 October
Halifax, Canada

Solution Mining Research Institute, Fall 2007 Technical Meeting
Halifax, Canada, October 7-10, 2007

Effect of natural convection on the blanket dissolution rate in a salt cavern

Mehdi Karimi-Jafari[1], Benoît Brouard[2], Pierre Bérest[1]

[1] LMS, Ecole Polytechnique, Palaiseau, France
[2] Brouard Consulting, Paris, France

ABSTRACT

In a paper presented during the SMRI 2006 Fall Meeting in Rapid City, the authors suggested that, before abandonment, a small quantity of gas be injected in the cavern to increase cavern compressibility and to prevent pressure build-up from being too severe. This solution proved to be robust in that a gas leak can be beneficial, making pressure build-up even slower than when gas remains trapped in the cavern.

In this paper the effect of brine convection on gas dissolution rate is discussed. It is proved that brine convection is driven by density changes induced by non-uniformity in brine temperature and by gas dissolution. Numerical computations considering both phenomena are performed, and different cavern shapes are considered. Two thermal loadings are discussed: (1) cavern brine temperature is lower than rock mass temperature by 3 °C ; and (2) globally, cavern brine is in thermal equilibrium with the rock mass (no temperature difference). The influence of the area of the gas/brine interface is discussed. The characteristic times of gas dissolution in these two cases are compared.

Keywords: Abandonment, Natural convection, Gas dissolution

1 INTRODUCTION

1.1 Main factors in the long-term behaviour of a sealed cavern

The long-term evolution of brine pressure in a sealed and abandoned cavern is governed by five main factors:

(1) brine warming and brine thermal expansion;

(2) cavern creep closure;

(3) brine (micro) permeation through the cavern walls;

(4) (possible) leaks through the plugged and cemented well; and

(5) cavern compressibility.

(Phenomena (1-4) result in cavern or brine-volume changes that are related to the cavern pressure change through cavern compressibility.)

When brine warming is negligible, an equilibrium pressure is reached when cavern creep closure (which leads to pressure build-up in a closed cavern) exactly equals brine permeation toward the rock mass plus possible leaks. This notion has been proven by two SMRI-supported in-situ tests (Bérest et al., 2001; Brouard et al., 2006).

Brine warming raises the most difficult issues. Brine warming originates from the temperature difference between the rock temperature and the cavern brine temperature that exists before the cavern is sealed. In general, brine is colder than rock. After cavern sealing, heat slowly is transferred from the rock mass to the cavern brine, and the brine gently warms to reach equilibrium with the rock mass. Brine warming is

more intense when the initial temperature difference, which is dependent on cavern depth and cavern history, is greater. The brine warming rate is faster in a smaller cavern. Brine warming generates the thermal expansion of the brine and the pressure build-up in a closed cavern. In sharp contrast with the effects of creep closure alone, brine warming plus creep closure can cause the pressure to build up to figures larger than geostatic ("overburden" or "lithostatic") pressure, leading to possible hydro-fracturing and the pollution of shallow water-bearing strata (Figure 1).

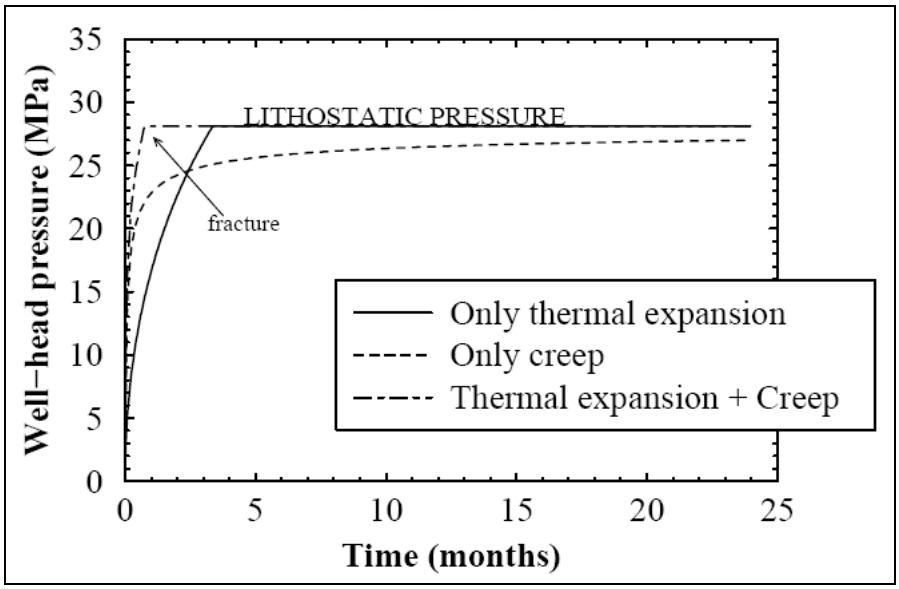

Figure 1 - Computed pressure evolution in a closed cavern. Brine thermal expansion leads to fracture (Brouard, 1998).

1.2 Waiting period

In some cases, such a scenario simply can be alleviated by waiting for some time before sealing the cavern. During the waiting period, a significant part of the temperature difference resorbs, and brine warming effects become sufficiently small to allow safe cavern sealing. Unfortunately, such an option is not realistic when a large and deep cavern is considered. In such a case, the waiting period can be several decades long.

1.3 Increasing cavern compressibility

Increasing cavern compressibility is another option. The cavern compressibility is the inverse of the stiffness of the (cavern + fluid stored in the cavern) system. The cavern compressibility is relatively small, because brine is a stiff body (much stiffer than gas), and the cavern compressibility factor generally is in the range 3.5 to 5×10^{-4} /MPa (Bérest et al., 1999) — i.e., approximately 3×10^{-6}/psi (Blair, 1998). This means that a temperature increase of 1°C, which leads to a relative increase of $\alpha_b = 4.4\times10^{-4}$ /°C in brine volume when the cavern is opened, will lead to brine pressure build-up of (approximately) $\beta/\alpha_b \approx 1$ MPa/°C in a closed cavern. This figure explains why brine warming has a dramatic effect on cavern pressure. However, cavern compressibility can be increased easily by injecting a small amount of gas before sealing the cavern (Figure 2). Carbon dioxide, which is inert and inexpensive, is a good candidate. (However, the possible aggressive effect of CO_2-saturated brine on steel casings and packers should be discussed.) Equations that describe pressure evolution in a cavern whose compressibility was lowered were discussed in Bérest et al. (2006), in which several examples were given and in which the following was proved.

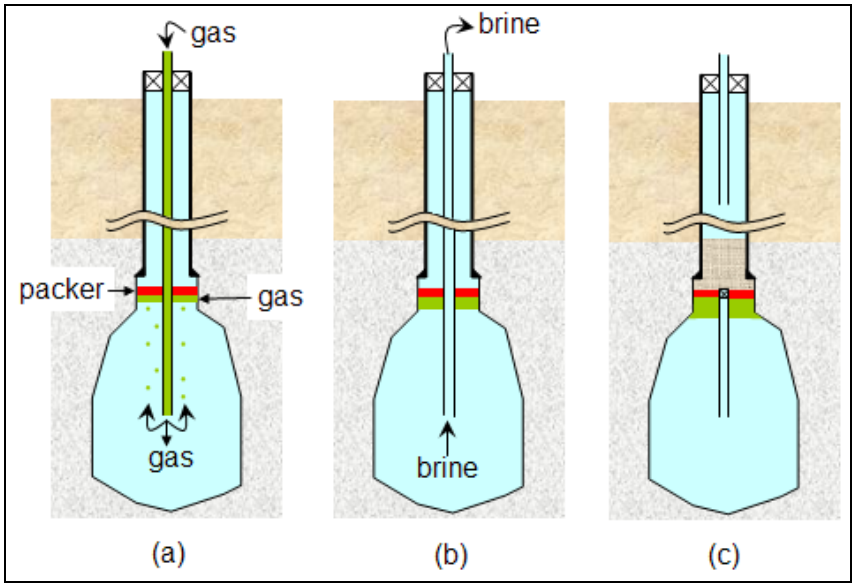

Figure 2 - Increasing cavern compressibility: (a) gas is injected below the packer; (b) brine is withdrawn to release pressure build-up; (c) the central tubing is sealed and cement is poured into the well.

1. The dissolution of CO_2 in brine, which acts as a leak, is favourable. It offers more room for the thermal expansion of brine and prevents fast cavern pressure build-up.
2. The "waiting period" option and the "compressibility increasing" option can be combined conveniently. A waiting period of 2-3 years allows a smaller amount of gas to be injected into the cavern than would be when the cavern sealed without a waiting period. The duration of the "waiting period" can be optimized on a case-by-case basis.

2 BRINE CONVECTION

In a paper presented during the SMRI 2007 Spring Meeting in Basel (Karimi-Jafari et al., 2007), steady-state convection in a brine-filled cavern was discussed. In fact, due to the natural geothermal gradient, warmer brine at the bottom of a cavern is slightly less dense than colder brine at the top, and a brine cavern is the seat of perennial convective flow. The authors pointed out that one or several convective cells develop; they stir cavern brine and make the brine temperature gradient in the cavern smaller than the geothermal gradient.

The objective of this paper is to highlight the coupled effect of brine convection on the gas dissolution rate. It should be noted that, in this case, brine convection is driven by two phenomena:

(1) density change induced by non-uniformity in brine temperature, which is responsible for thermal convection; and

(2) density change induced by gas dissolution, which, therefore, is called the mass transfer phenomenon.

The process is coupled in that convection rapidly transports brine, which is unsaturated with respect to gas, to the top of the cavern, considerably increasing the gas dissolution rate.

In other words, at the cavern top, gas dissolves into brine, which becomes heavier and drops, providing room for deeper brine that contains less dissolved gas and is lighter. The convection induced by the mass transfer phenomenon is more effective when the concentration at saturation of the gas contained in the top of the cavern in the brine is larger. These two convective phenomena combine, yielding to faster gas dissolution rate.

In this paper, the selected gas blanket is carbon dioxide. The CO_2 equilibrium concentration in brine is especially large and reaches 1.2 kmole/m^3 at 27 °C and 5 MPa.

Brine flow equations considering both phenomena are as follows:

$$\begin{cases} div\vec{u} = 0 \\ \dfrac{\partial c}{\partial t} + \overrightarrow{grad}\left[c \cdot \vec{u} - k^{diff} \overrightarrow{grad}(c) \right] = 0 \\ \dfrac{\rho_f}{1-c}\dfrac{d\vec{u}}{dt} = -\overrightarrow{grad}\left(P - \dfrac{\rho_f g z}{1-c} \right) + \mu_f \Delta\vec{u} - \dfrac{\alpha_f \rho_f \theta_f}{1-c}\vec{g} \\ \dfrac{\partial \theta_f}{\partial t} + \left[\left(\dfrac{dT_\infty}{dz} \right) \cdot \vec{e}_z + \overrightarrow{grad}\ \theta_f \right] \cdot \vec{u} = k_f^{th} \Delta\theta_f \end{cases} \tag{1}$$

where P is the fluid pressure,

ρ_f is the fluid density,

$\vec{u}$ is the fluid velocity,

μ_f is the dynamic viscosity of the fluid,

α_f is the thermal expansion coefficient of the fluid,

k_f is the thermal diffusivity of the fluid,

k^{diff} is the diffusivity coefficient of gas in the fluid,

θ_f is the difference between fluid temperature and geothermal temperature at the mesh top, and

c is the mass concentration of gas in the fluid.

Within the rock mass, the Fourier equation holds:

$$\begin{cases} \dfrac{\partial \theta_R}{\partial t} = k_R \Delta\theta_R \\ K_f \left.\dfrac{\partial \theta_f}{\partial n}\right|_f = K_R \left.\dfrac{\partial \theta_R}{\partial n}\right|_R \quad \text{at cavern wall} \end{cases} \tag{2}$$

where θ_R is the difference between the disturbed temperature of the rock T and the geothermal temperature T_∞ at rock depth,

k_R is the rock thermal diffusivity, and

K_f and K_R are the fluid and rock thermal conductivities, respectively.

This set of equations was solved numerically using the *Adina CFD* code for various cavern shapes. Turbulent flow is considered using the k-ε standard model.

Four different cases were considered (Table 1 and Figure 3). Zero temperature was set at mesh top, and a vertical temperature gradient, dT_∞/dz (geothermal gradient), was set on the right-hand boundary. The relative temperature of the rock mass at cavern average depth, θ_R, is presented in Table 1 for different cases. It should be noted that, to obtain the actual temperature at any depth, the geothermal temperature at the mesh top must be added to the computed temperature. θ_f^0 is the initial temperature difference between the cavern fluid and the rock mass at the mesh top.

Table 1 - Considered cavern parameters.

Case #	Cavern shape	Radius (m)	Height (m)	$\frac{dT_\infty}{dz}$ (°C/m)	θ_R (°C)	θ_f^0 (°C)
1	Cylindrical cavern	15	6	0.01	0.25	0.25
2	Cylindrical cavern	15	6	0.01	0.25	-3.0
3	Spherical cavern	10	20	0.01	0.4	0.4
4	Spherical cavern	10	20	0.01	0.4	-3.0

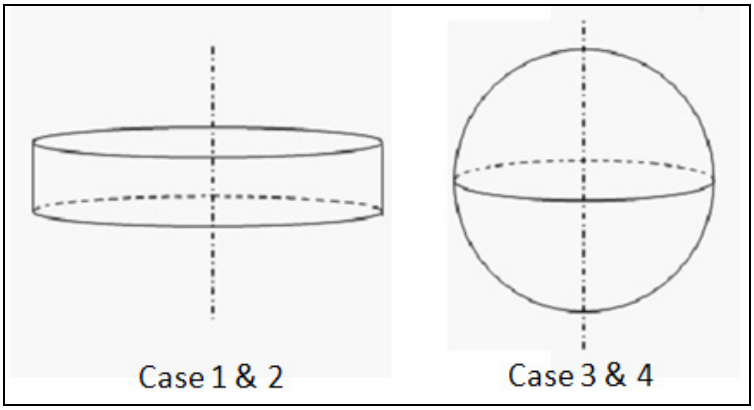

Figure 3 - Considered cavern shapes.

At time 0, a small quantity of CO_2 is injected at the top of the cavern. The gas blanket is simulated by applying a constant gas concentration at the cavern top. The CO_2 mass concentration at saturation is assumed to be $c_s = 0.044$ (at 27°C and 5 MPa).

We define here the characteristic time of the dissolution rate as a time after which the minimum gas concentration in the cavern is one-fourth the concentration at saturation ($c_{\min} = c_s/4$). This characteristic time provides an index of the completeness of the dissolution process. The characteristic times of the gas dissolution are compared in various cases.

Case 1 — Cylindrical cavern with no initial temperature difference

In this case, a cylindrical cavern is considered, and the initial brine temperature is equal to the geothermal temperature at cavern average depth. It is assumed that the gas blanket has been spread uniformly at the top of the cavern. Numerical computations show that, in this case, the characteristic time of the dissolution process is $t_c^{diss} = 39$ days. Gas concentration, brine temperature and brine velocity distribution at this time ($t = t_c^{diss}$) are illustrated on Figures 5 to 7, respectively.

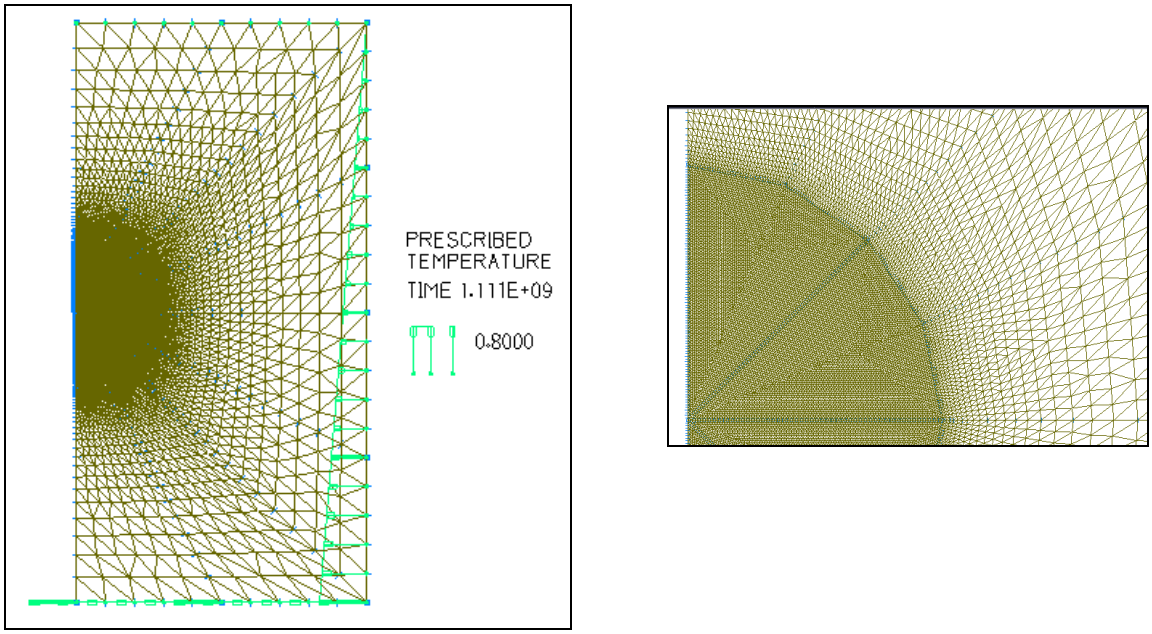

Figure 4 - Example of a mesh used in the *Adina CFD* code (Case 3) — Whole mesh (left) and close-up (right). There are 43,352 elements and 21,827 nodes.

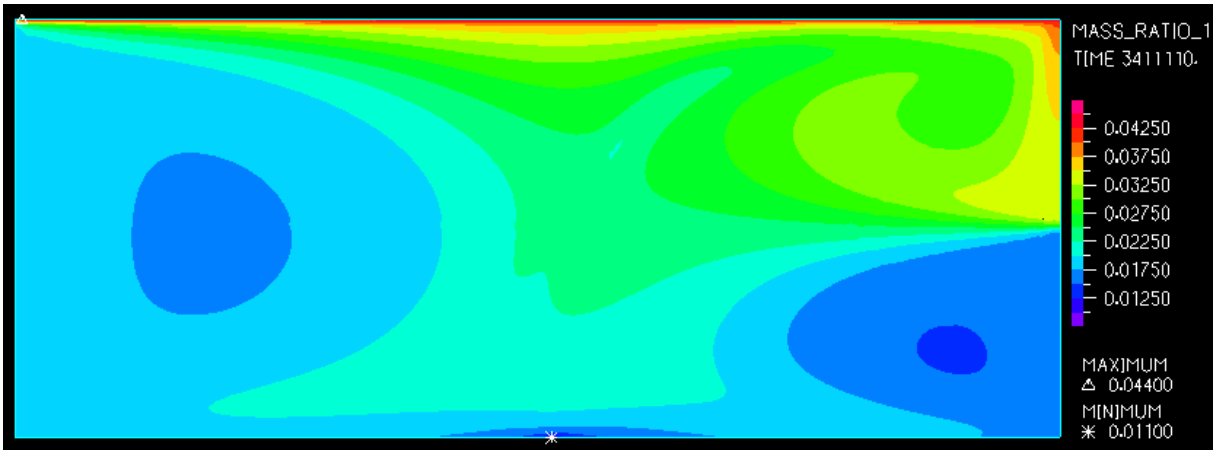

Figure 5 - Gas concentration distribution at 39 days in case 1.

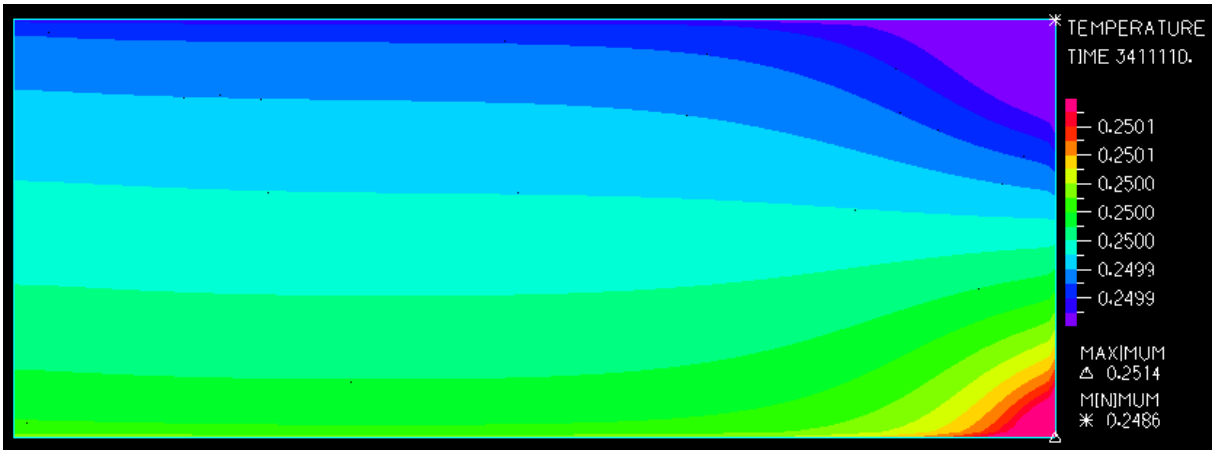

Figure 6 - Brine temperature distribution at 39 days in case 1.

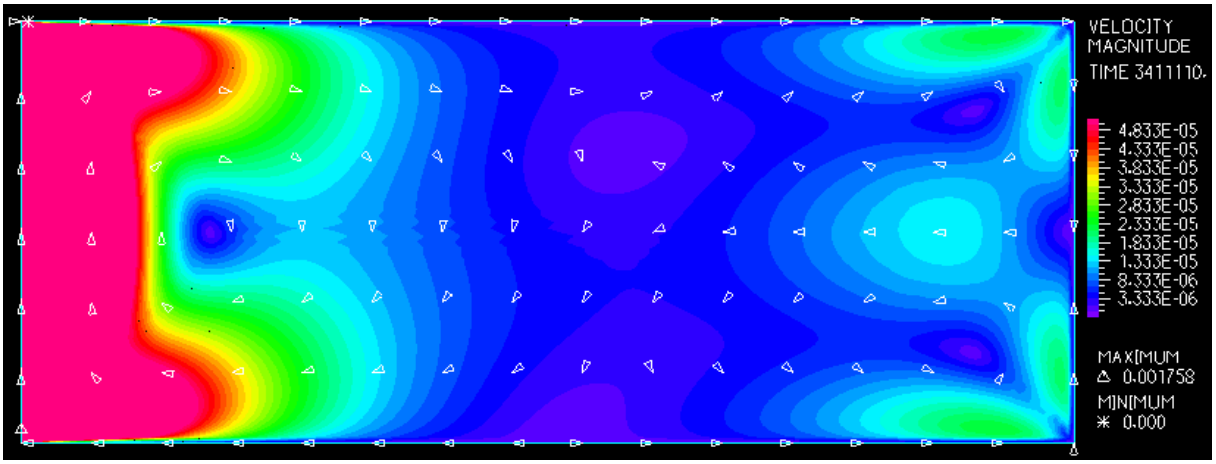

Figure 7 - Brine velocity magnitude (in m/s) at 39 days in case 1.

Case 2 — Cylindrical cavern with initial temperature difference

In this case, a cylindrical cavern is considered in which the initial brine temperature in the cavern is colder than the geothermal temperature at the mesh top by 3 °C, making thermal convection in the cavern more effective than in case 1. It is assumed that gas has been spread uniformly at the cavern top. In this case, numerical computations prove that the characteristic time is equal to $t_c^{diss} = 2.6$ hours. It is seen that the natural convection is accelerated dramatically by even a small temperature difference. Gas concentration, brine temperature and brine velocity distribution at $t = t_c^{diss}$ are illustrated on Figures 8 to 10, respectively.

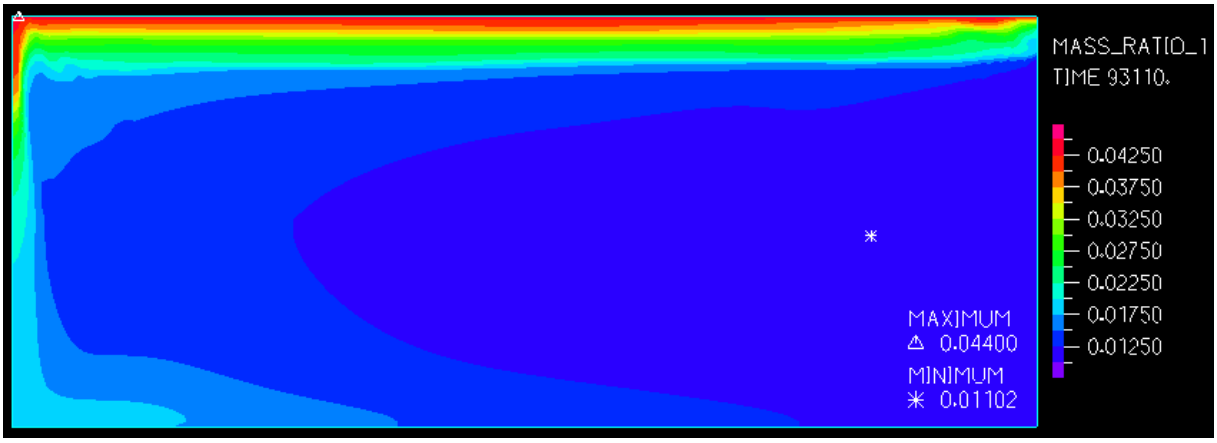

Figure 8 - Gas concentration distribution at 2.6 hours in case 2.

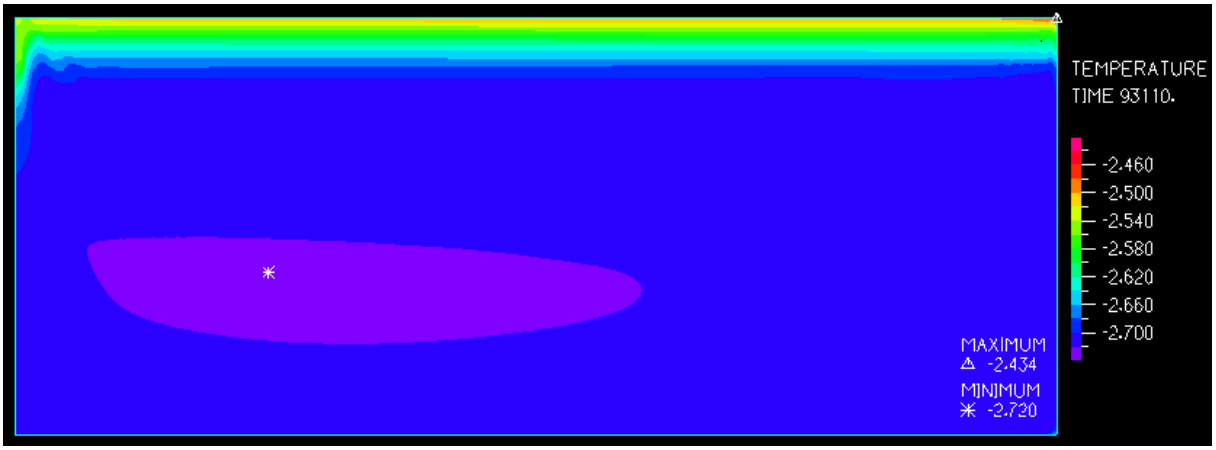

Figure 9 - Brine temperature distribution at 2.6 hours in case 2.

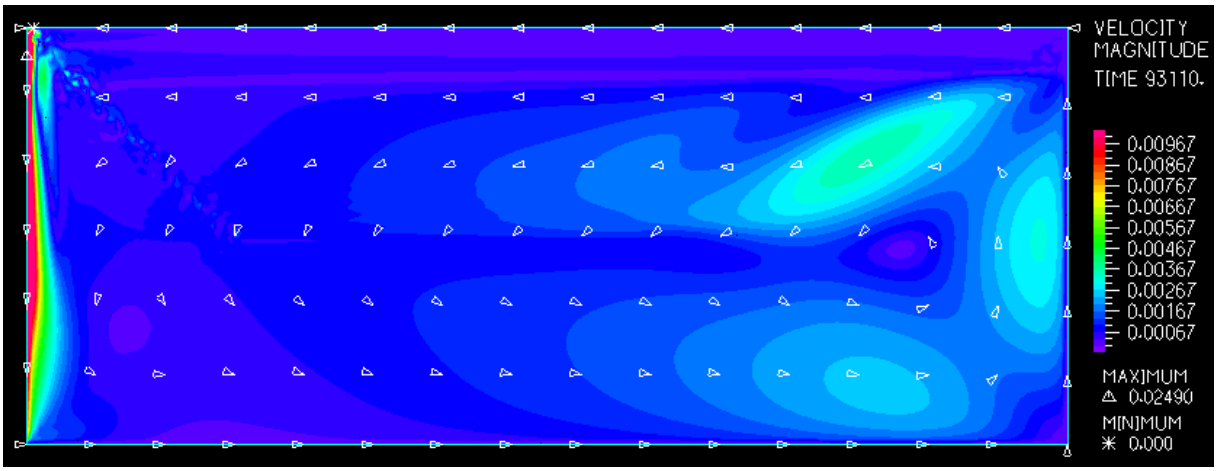

Figure 10 - Brine velocity magnitude (in m/s) at 2.6 hours in case 2.

Case 3 — Spherical cavern with no initial temperature difference

In this case, a spherical cavern is considered, and the initial brine temperature is equal to the geothermal temperature at cavern average depth. The gas blanket is assumed to be spread on a small surface at the cavern top. (The gas/brine interface area is much smaller than in the former case.) Numerical computations show that, in this case, the characteristic time for the dissolution process is $t_c^{diss} = 116$ days. Gas concentration, brine temperature and brine velocity distribution at $t = t_c^{diss}$ are illustrated on Figure 11.

Case 4 — Spherical cavern with initial temperature difference

In this case, a spherical cavern is considered in which the initial brine temperature in the cavern is colder than the geothermal temperature at the mesh top by 3 °C. Numerical computations prove that, here, the characteristic time is equal to $t_c^{diss} = 6$ days. Gas concentration, brine temperature and brine velocity distribution at $t = t_c^{diss} / 2 = 3$ days are illustrated on Figure 12.

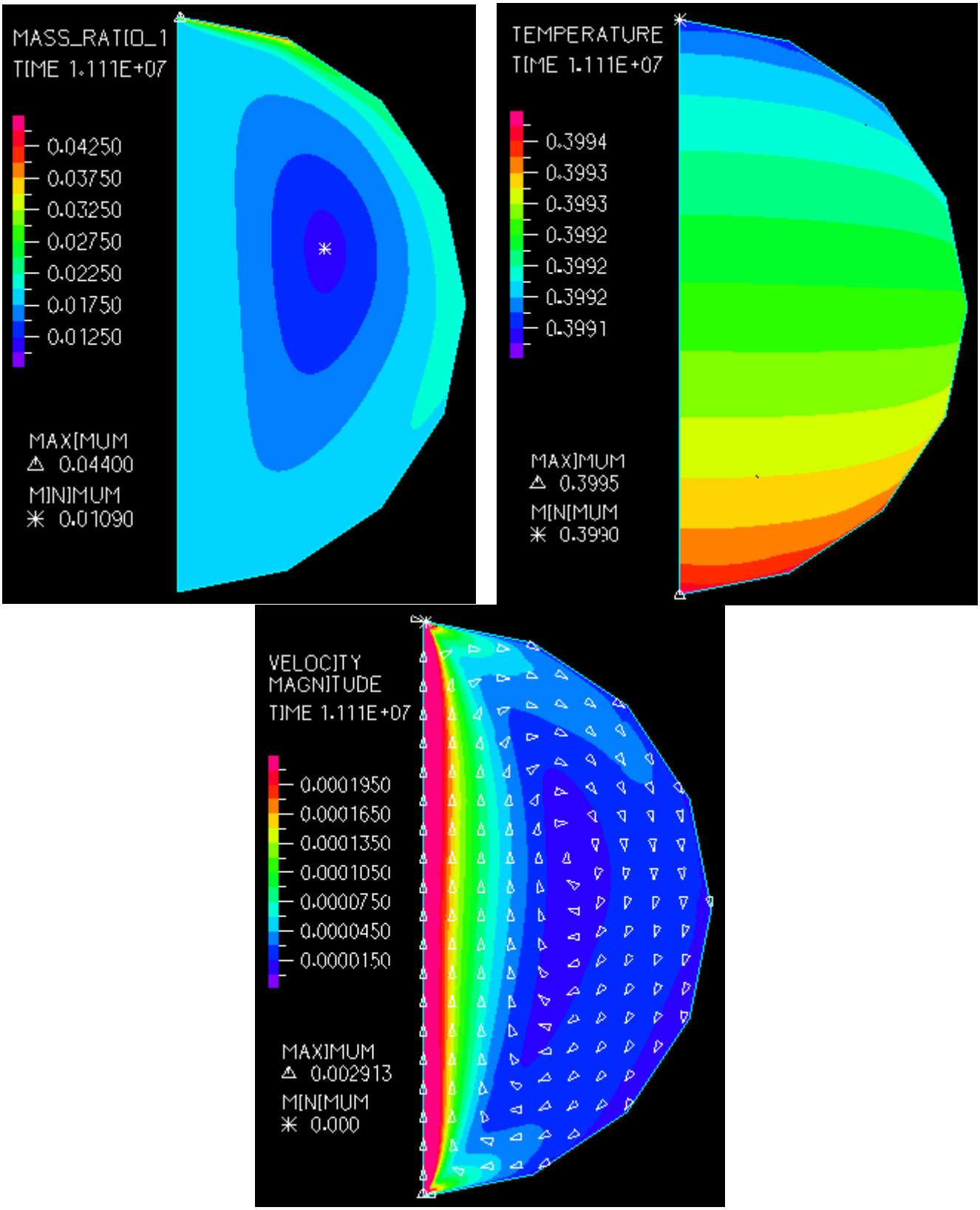

Figure 11 - Case 3, gas concentration (top left), brine temperature (top right), and velocity magnitude (bottom) at 116 days.

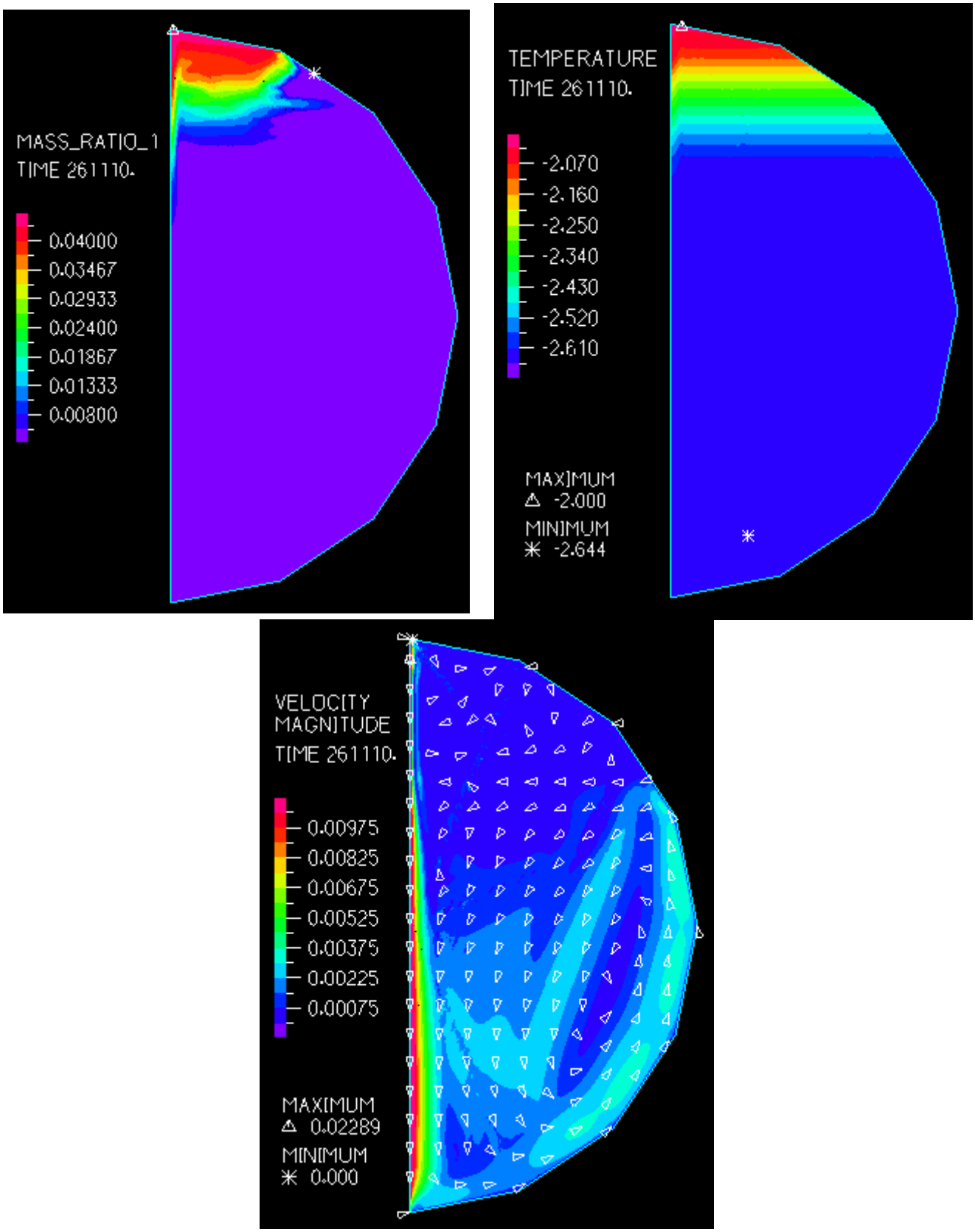

Figure 12 - Case 4, gas concentration (top left), brine temperature (top right), and velocity magnitude (bottom) at 3 days.

CONCLUSIONS

A model of brine convection in a salt cavern accounting for thermal and mass transfer phenomena was presented. The blanket dissolution rate was observed to be influenced strongly by brine velocity. Brine flow is extremely sensitive to the initial temperature difference between the cavern brine and rock mass, and to the area of the gas/brine interface. Brine natural convection in a sealed cavern containing a gas blanket accelerates the gas dissolution process. It has a beneficial effect on pressure evolution of the sealed cavern.

REFERENCES

Bannach A., Wagler T., Walden S., Klafki M., Köckritz V., Mulkamanov A. and Kneer A. *Technology enhancements for (1) inventory assessment and mechanical integrity testing of gas-filled solution mined caverns and (2) mechanical integrity tests of solution mining and liquid storage caverns*. Report prepared for the Gas Research Institute, Ref. GRI-05/0175, 73 pages (2005).

Bérest P, Bergues J, Brouard B. *Review of static and dynamic compressibility issues relating to deep underground salt caverns*. Int. J. Rock Mech. Min. Sc., Vol.36 (8), pp. 1031–49 (1999).

Bérest P., Bergues J., Brouard B., Durup J.G. and Guerber B. *A salt cavern abandonment test*. Int. J. Rock Mech. Min. Sc., Vol.38 (3), pp. 357-368 (2001).

Bérest P., Karimi-Jafari M., Brouard B. and Durup G. Brine warming in a sealed cavern: what can be done? Proc. SMRI Fall Meeting, Rapid City (2006).

Blair R.W. *Mechanical Integrity Test (MIT) Nitrogen Interface Method*. SMRI Short Course, SMRI Spring Meeting, Houston (1998).

Brouard (1998). On the behaviour of salt cavern – Theorethical study and in situ experiments. PhD Thesis, Ecole Polytechnique, France (1998).

Brouard Consulting, Institute für Unterirdishches Bauen (IUB), Ecole Polytechnique, Total E&P France, Géostock (2006). *Salt-Cavern Abandonment Field Test in Carresse*. SMRI RFP 2003-2-B, Final Report (2006).

Karimi-Jafari M., Bérest P. and Brouard B. *Thermal effects in salt caverns*. Proc. SMRI Spring Meeting, Basel, pp. 165-177 (2007).

Markatos N. C. and Pericleous K. A. *Laminar and turbulent natural convection in an enclosed cavity*. Int. J. Heat Mass Transfer, Vol.27, No.5, pp.755-772 (1984).